Effect of Time Step Size in MM5 Simulations of a Mesoscale Convective System

MEI XU

Program in Atmospheric and Oceanic Sciences, University of Colorado, and National Center for Atmospheric Research, Boulder, Colorado

JIAN-WEN BAO

Cooperative Institute for Research in Environmental Sciences, University of Colorado, and NOAA/Environmental Technology Laboratory, Boulder, Colorado

THOMAS T. WARNER

Program in Atmospheric and Oceanic Sciences, University of Colorado, and National Center for Atmospheric Research, Boulder, Colorado

DAVID J. STENSRUD

NOAA/National Severe Storms Laboratory, Norman, Oklahoma

(Manuscript received 7 January 2000, in final form 20 July 2000)

ABSTRACT

Results from simulations of a mesoscale convective system (MCS) that occurred in a weakly forced large-scale environment show significant sensitivity to the time step size chosen for model integration. As the time step is decreased, the movement and longevity of the simulated MCS depart further from the observations. It is found that the time step–dependent formulation of the numerical diffusivity is responsible for a major part of this sensitivity in the simulated MCS. The changes contributed by truncation errors may or may not be negligible, depending on the physics schemes used in the simulations. This suggests that the choice of a specific linearly stable model time step, in combination with the definition of the numerical diffusivity, may at times be as important as the choice of the basic model configuration.

1. Introduction

A mesoscale convective system (MCS) is an organized region of convective activity that often has a leading convective line followed by a trailing zone of stratiform precipitation (Houze 1993). Due to uncertainties in simulating local forcing that acts to initiate convection, numerical models have difficulty predicting MCSs in the correct location and at the correct time (Heideman and Fritsch 1988). Two types of uncertainty have long been recognized by the scientific community: 1) initial condition error, which for MCS simulations is often due to the lack of mesoscale features in the model initialization (Stensrud and Fritsch 1994a,b), and 2) postinitial model error, as evidenced by the uncertainties in the parameterization schemes that are used in the models (e.g., Emanuel and Raymond 1992; Mellor and Yamada 1982; Walcek 1994).

Compared to those two sources of error, the choice of a time step for model integration is generally thought to be much less important and less likely to produce significant error. That is, the choice of time step is not expected to significantly affect the simulation, as long as the model remains numerically stable. In addition, due to the vast amount of work entailed, it is virtually impossible to provide a precise estimate of the temporal discretization errors. The time step has to be selected by what is essentially ''trial and error.'' Generally speaking, the selection of a time step is a compromise between numerical accuracy and computational cost.

However, since highly nonlinear processes are involved in the simulation of MCSs, there is a likelihood that the cumulative effect of small errors from the discrete temporal integration during the early simulation hours can become amplified later in the simulation. Therefore, the time step size may play a more important role than is usually expected. To determine the effect

Corresponding author address: Dr. Mei Xu, Research Applications Program, National Center for Atmospheric Research, P.O. Box 3000, Boulder, CO 80307.
E-mail: meixu@ncar.ucar.edu

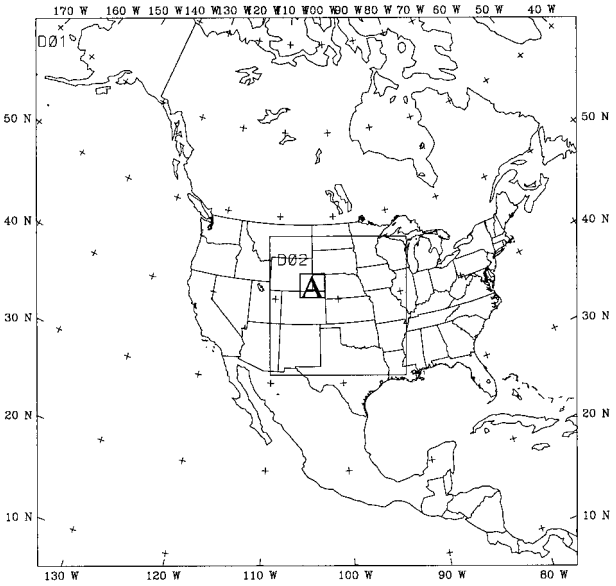

FIG. 1. Domain configuration for the MM5 simulations. The letter A marks the area of convective initiation on 27 May 1985.

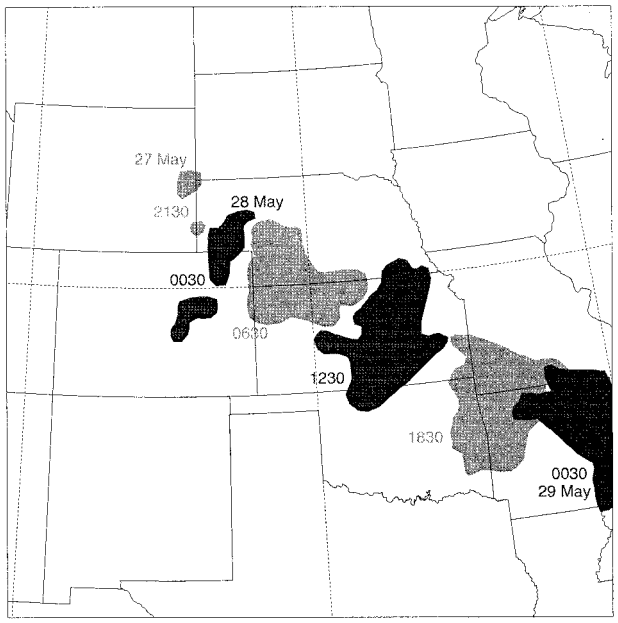

FIG. 2. Observed MCS reflectivity pattern, as indicated by the national radar summaries, from initiation at 2130 UTC 27 May through demise at 0030 UTC 29 May 1985. The MCS consists of a leading-edge convective line, typically located on the southeastern flank, followed by a trailing stratiform precipitation region to the northwest.

of time step size in the simulation of MCSs, several numerical experiments are conducted using different time step sizes in a mesoscale model.

This paper shows a few examples of the sensitivity to the time step during the simulation of an MCS that occurred in a weakly forced large-scale environment. Some reasons for this sensitivity are suggested and discussed. Results using several different model configurations are presented, since the MCS simulation may be sensitive to model physics schemes. The focus of the experiments is not on the absolute predictive skill of the simulations but on how the simulations may be affected by changing the time step size. The numerical model configurations used are discussed in section 2, and section 3 provides a brief overview of the meteorological event. Section 4 contains the numerical model results, with a final discussion in section 5.

2. Numerical model configurations

The numerical experiments are conducted using the Pennsylvania State University–National Center for Atmospheric Research (Penn State–NCAR) fifth-generation Mesoscale Model (MM5; Dudhia 1993; Grell et al. 1994). A two-way interactive nested grid is used for all of the simulations (Fig. 1). The outer mesh has $96 \times 96 \times 23$ grid points with a horizontal grid resolution of 75 km, while the inner mesh has $73 \times 73 \times 23$ points and a grid resolution of 25 km. The 23 sigma levels are spaced so as to provide much higher vertical resolution in the planetary boundary layer (PBL) than at upper levels.

The initial and boundary conditions for the simulations are generated using the standard static initialization procedure for MM5. First-guess fields are produced by interpolating the National Centers for Environmental Prediction (NCEP) 2.5° latitude–longitude global analyses to the outer computational grid, using two-dimensional 16-point overlapping parabolic fitting. Standard upper-air and surface observations are then used to adjust the NCEP analysis through a successive-correction type of objective analysis (Benjamin and Seaman 1985). The mean divergence in the column is removed, and the meteorological fields are interpolated from the outer grid to the inner grid points.

All simulations use the Blackadar PBL scheme (Zhang and Anthes 1982; Blackadar 1979) and the resolvable-scale microphysics of Dudhia (1989). Two different convective parameterization schemes (CPSs), the Grell scheme (Grell 1993) and the Betts–Miller scheme (Betts and Miller 1993; Janjic 1994), are tested. A second-order horizontal diffusion term is used adjacent to the lateral boundaries, while a fourth-order horizontal diffusion term is used on the other interior grid points. The horizontal diffusion coefficient consists of a background value and a term proportional to the deformation. Further information on the model system can be found in Stensrud et al. (2000). The simulations, each 48 h long, are initialized at 1200 UTC 27 May 1985.

3. Case description

National radar summaries show that a thunderstorm started at 1900 UTC 27 May 1985 along the high plains

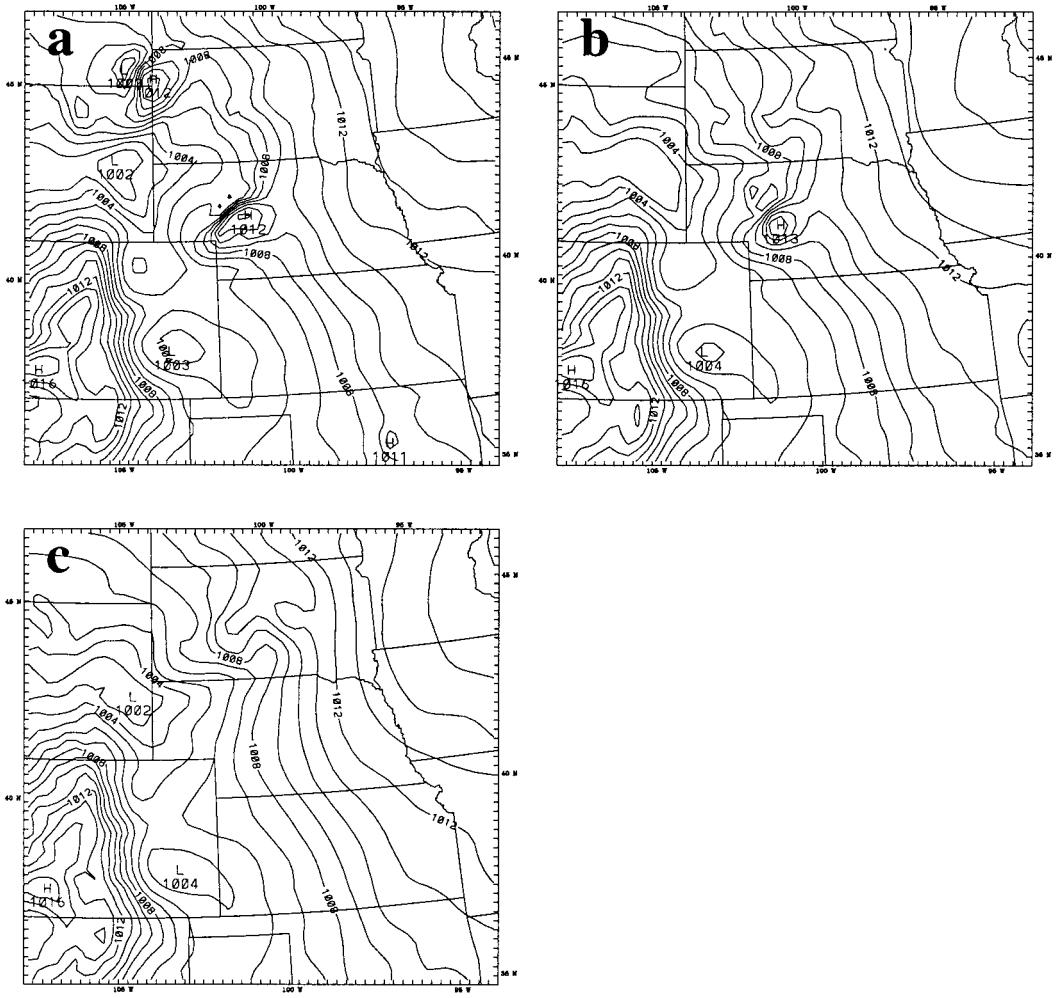

FIG. 3. Sea level pressure fields at 18 h for the HYGR runs: (a) $\Delta t = 225$ s, (b) $\Delta t = 150$ s, and (c) $\Delta t = 75$ s. Please note that only part of the inner domain is plotted.

of eastern Wyoming, developed into an MCS over the next 6 h, and then moved southeastward over the next 18 h as it crossed Kansas, skirted the far northeastern corner of Oklahoma and moved into Arkansas (Fig. 2). The MCS was located in eastern Arkansas by 0000 UTC 29 May, and then finally decayed as it moved southeastward into Mississippi. This MCS qualified as a mesoscale convective complex (MCC); (Maddox 1980) and was the longest-lived MCC during 1985 over the United States (Augustine and Howard 1988).

A particularly interesting aspect of this MCS is that it was located beneath a large-scale ridge in association with large-scale subsidence (Stensrud et al. 2000). With the strong capping inversion that is suggested by the morning soundings (lid strength index values of 2°–5°C) and no large-scale upward motion to reduce the inversion strength, significant mesoscale forcing is required to initiate convection. Observations indicate that the initial thunderstorm was initiated along the dryline, where significant mesoscale ascent is typically produced. Owing to the lack of large-scale forcing, this case represents a difficult forecast situation. Unfortunately, it is fairly representative of the type of late spring or summertime convective event routinely handled by operational forecasters. Accurate quantitative precipitation forecasts (QPFs) for such events are usually extremely challenging (see Heideman and Fritsch 1988).

More details of the event are given by Stensrud et al. (2000), who also show that the MM5 simulation of the event is sensitive to both the model physics and the initial conditions. The sensitivity to the physics options led us to examine the sensitivity to time step size using more than one model configuration.

4. Model results

Three experiments are conducted, using a different MM5 configuration for each: the hydrostatic MM5 with the Grell CPS (HYGR), the nonhydrostatic MM5 with the Grell CPS (NHGR), and the nonhydrostatic MM5

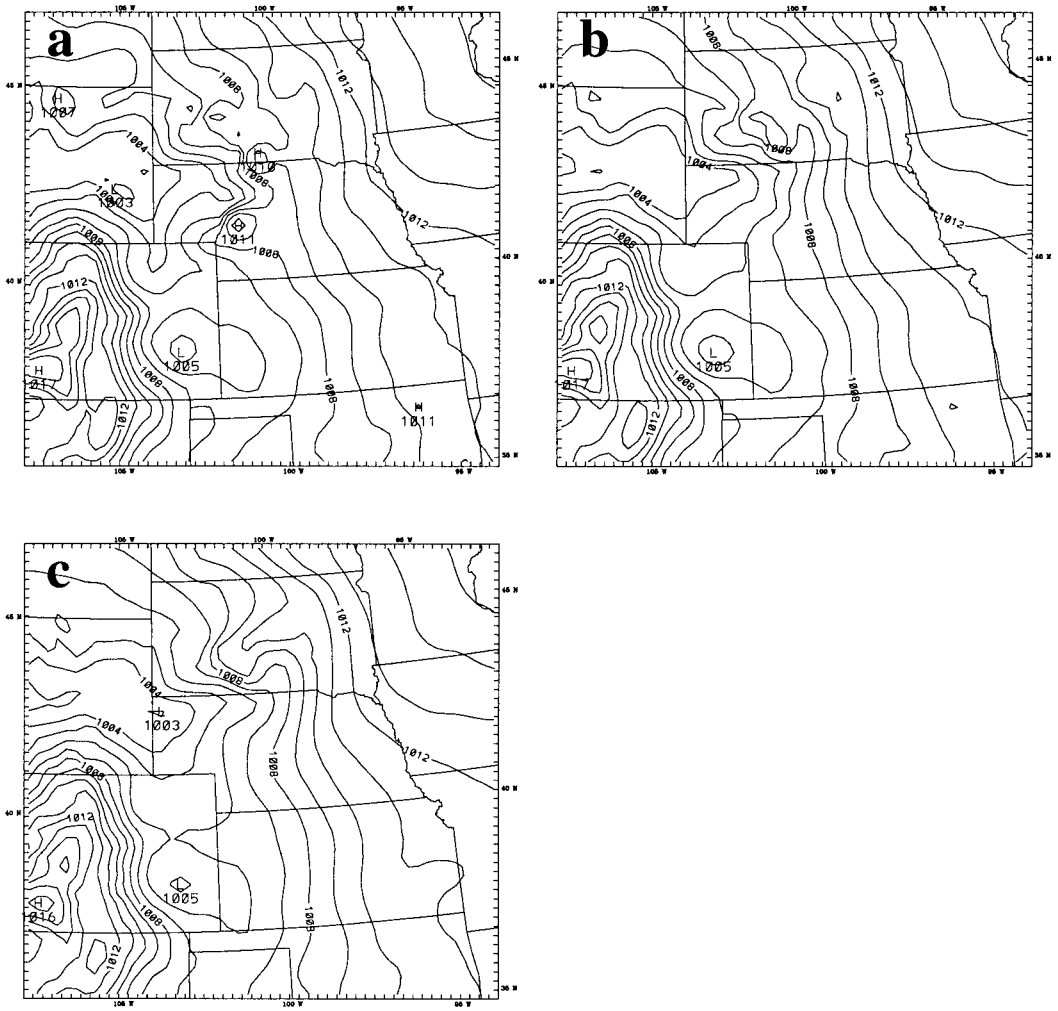

FIG. 4. Sea level pressure fields at 18 h for the NHGR runs: (a) $\Delta t = 225$ s, (b) $\Delta t = 150$ s, and (c) $\Delta t = 75$ s.

with the Betts–Miller CPS (NHBM). The sensitivity of model forecasts to time step size is tested by repeating each of the three simulations using different time steps. Typically, a time step of $3\Delta X$ (in seconds, with ΔX in kilometers) is recommended for use with MM5. In each of the three experiments, three model runs are performed using different time steps for the outer grid: 1) $\Delta t = 225$ s (equivalent to the recommended $\Delta t = 3\Delta X$), 2) $\Delta t = 150$ s, and 3) $\Delta t = 75$ s. The time step used on the inner grid is one-third of the time step on the outer grid. Therefore, a total of nine simulations are produced and evaluated.

In all the simulations, the same initial conditions are used and the size of the grid increment is held constant. In this paper, the MM5 runs are identified by the CPS and the outer grid time step used in the integration, for example, run HYGR150 refers to the hydrostatic run using the Grell CPS and an outer grid time step $\Delta t = 150$ s.

a. Convective initiation, evolution, and dissipation

All nine simulations show convective initiation over the Wyoming–Nebraska–Colorado region between 9 and 15 h after the model initialization, but the exact location of initiation and the subsequent evolution of the convection are different from run to run. For each model configuration, when the time step is changed, the location and intensity of the convection also change. The extent of the changes, that is, the degree of sensitivity of the simulation with respect to time step size, differs from one model configuration to another.

The hydrostatic run using the Grell CPS with $\Delta t = 225$ s (HYGR225) produces two well-defined MCSs, one moving eastward and the other moving southeastward (Fig. 3a). The eastward-moving MCS starts in northeast Wyoming at 9 h, and the southeastward-moving MCS starts at around 12 h in western Nebraska and moves across Kansas by 30 h. When the time step is reduced to 150 s (HYGR150), the convective activity

in northeast Wyoming at 12 h becomes much weaker and fails to develop further. Also, the southeastward-moving system is weak in HYGR150, as indicated by the smaller surface mesohigh at 18 h (Fig. 3b), and the convection dissipates by 24 h. When the time step is further reduced to 75 s (HYGR75), only one MCS develops, starting in western South Dakota at around 12 h and moving eastward (Fig. 3c). Since observations indicate that the one MCS that develops on this day was initiated in eastern Wyoming and moved southeastward across Kansas and into Arkansas (see Fig. 2), the model simulations actually worsen as the time step is decreased.

The nonhydrostatic run using the Grell CPS and $\Delta t = 225$ s (NHGR225; Fig. 4a) also produces two areas of convective activity that start between 12 and 15 h. Both convective regions move eastward, with the one to the south being rather weak and brief. Around 21 h, there is only one system left in the South Dakota–Nebraska border region. When the time step is reduced, the early convection to the south becomes even weaker and more short lived (Figs. 4b,c). In the NHGR75 run, the activity in southeast Wyoming and eastern Nebraska is reduced to some local convection around 12–15 h. This activity dissipates quickly, leaving only one convective region in central South Dakota at 18 h (Fig. 4c).

In contrast to the runs with the Grell CPS, all three nonhydrostatic simulations (with different time steps) using the Betts–Miller scheme produce two well-organized convective systems, one starting at ~9 h near the Wyoming–South Dakota border and the other starting in western Nebraska at ~12 h. Again, the northern system moves eastward and the southern system moves southeastward (Fig. 5). When the time step is reduced from 225 (Fig. 5a) to 75 s (Fig. 5c), the intensities of the two systems are reduced, but the paths and locations of the two systems are relatively little changed before their dissipation around 30–36 h.

b. Precipitation

In the HYGR experiments, the 225- and 150-s runs produce very different MCSs. As a consequence, the location and timing of the precipitation are very different in the two simulations (Fig. 6). The differences in rainfall rates produced by the three simulations are large, as the simulation with the largest time step size produces the largest 3-h precipitation totals. In addition, the 225-s run simulates moderate precipitation totals in southern and central Nebraska during 21–24 h (Fig. 6b), while the other two runs produce no precipitation in this same region (Figs. 6d,f). As the time step size is decreased, the precipitation from the northern MCS for 21–24 h extends farther and farther southward, as the southern MCS becomes weaker and weaker.

The simulated 3-h precipitation amounts at 15 and 24 h for the NHBM experiments indicate that the precipitation areas are similar among these simulations that use different time step sizes (Fig. 7). However, the intensities of the precipitation regions are rather different. When the time step is reduced from 225 to 150 s, the maximum precipitation amount produced over Nebraska between 21 and 24 h is decreased by 21% (cf. Figs. 7b,d). When the time step is further reduced from 150 to 75 s, no obvious convergence is seen as the precipitation maximum decreases further by 33% (cf. Figs. 7d,f). Similar results also occur in the NHGR experiments (not shown). A reduction of time step from 225 to 150 s results in moderate or significant changes in both the locations and the intensities of the simulated rainfall in the NHGR experiments.

c. Mesoscale structures

A few model variables other than the precipitation, such as the mean PBL temperature and 850-hPa vertical velocity in the area of convective initiation (area A in Fig. 1), are examined to determine their response to changes in time step sizes. The results show that, for the same model configuration, the differences in the simulated low-level temperatures are relatively small (Figs. 8a,c,e). When the time step changes from 225 to 150 s, the low-level temperatures change by less than 0.6 K, which is approximately 5% of the modeled range of variation of the variable. Similar small differences are seen in the values of vertical motion (Figs. 8b,d,f). Thus, the time step effect on the more fundamental model variables seems to be much smaller than the effect on the precipitation, which is undoubtedly the most difficult parameter to forecast correctly.

d. Partition of parameterized and grid-scale precipitation

A further examination of the precipitation is provided by partitioning the total precipitation into subgrid-scale precipitation (through parameterized convection); and grid-scale precipitation (through resolvable-scale processes). The grid-scale and parameterized rainfall during 21–24 h are shown for HYGR225, HYGR150, and HYGR75 in Fig. 9, and for NHBM225, NHBM150, and NHBM75 in Fig. 10. At the verification time, grid-scale rainfall dominates in the HYGR runs (Fig. 9), and the parameterized rainfall constitutes only a small fraction of the total rainfall. In contrast, in the NHBM runs (Fig. 10), the parameterized rainfall constitutes a much larger fraction of the total rainfall, especially for the southeastward-moving MCS. This result is consistent with the findings by Kuo et al. (1996) and Wang and Seaman (1997), who studied the ratios of subgrid-scale precipitation to total precipitation for various CPSs.

Both the parameterized and grid-scale precipitation show evident changes as the time step is changed. In HYGR75 (Figs. 9e,f), both the parameterized and grid-scale precipitation disappear in south-central Nebraska, the region where a southeastward-moving MCS pro-

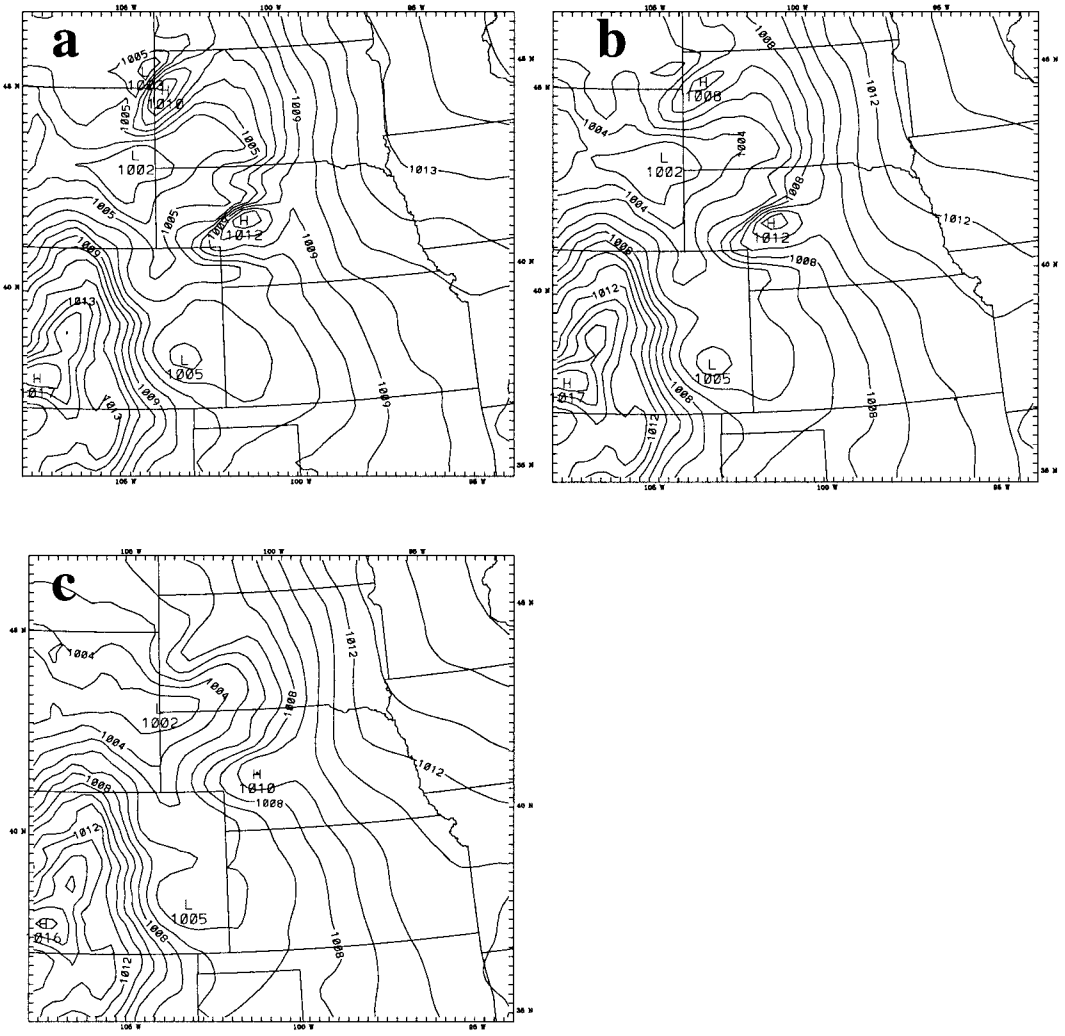

FIG. 5. Sea level pressure fields at 18 h for the NHBM runs: (a) $\Delta t = 225$ s, (b) $\Delta t = 150$ s, and (c) $\Delta t = 75$ s.

duces significant grid-scale rainfall in the HYGR225 run (Fig. 9a). In the NHBM runs (Fig. 10), as the time step is changed from 225 to 75 s, the grid-scale precipitation in south-central Nebraska also largely disappears, while 65% of the parameterized rainfall in the region remains. The nonlinear interactions between the explicit and implicit precipitation schemes make it difficult to determine which scheme is more time step dependent.

These results, together with those described in section 4b, indicate that in all three of the model configurations tested the evolution of the precipitation field is sensitive to the time step. This sensitivity is seen in both the parameterized and grid-scale precipitation fields. Sensitivity of the more fundamental model variables is much smaller, but still discernible. Sensitivities using other configurations of MM5 with different CPSs, PBL schemes, microphysical schemes, etc. have not been examined. Nevertheless, in all three experiments, the precipitation differences caused by time step changes are large.

5. Effect of horizontal diffusivity

The explicit and parameterized precipitation schemes in MM5 are, by nature, functions of the prognostic model variables. The results indicate that variation of the basic model predictands with time step size leads to significant changes in the evolution of the MCS, especially in the precipitation fields. This sensitivity may indicate that the precipitation schemes used in this study are highly nonlinear with respect to small changes in the prognostic model variables. It may also be due to numerical discretization of model physics as suggested by Janssen and Doyle (1997), or due to the interaction of the precipitation schemes with numerical terms (such as numerical dissipation) that are dependent on time step.

In general, the modest responses of the prognostic variables to changes in time step size (Fig. 8) may be considered as consisting of two parts. One part is related to the truncation error that is due to discretization in

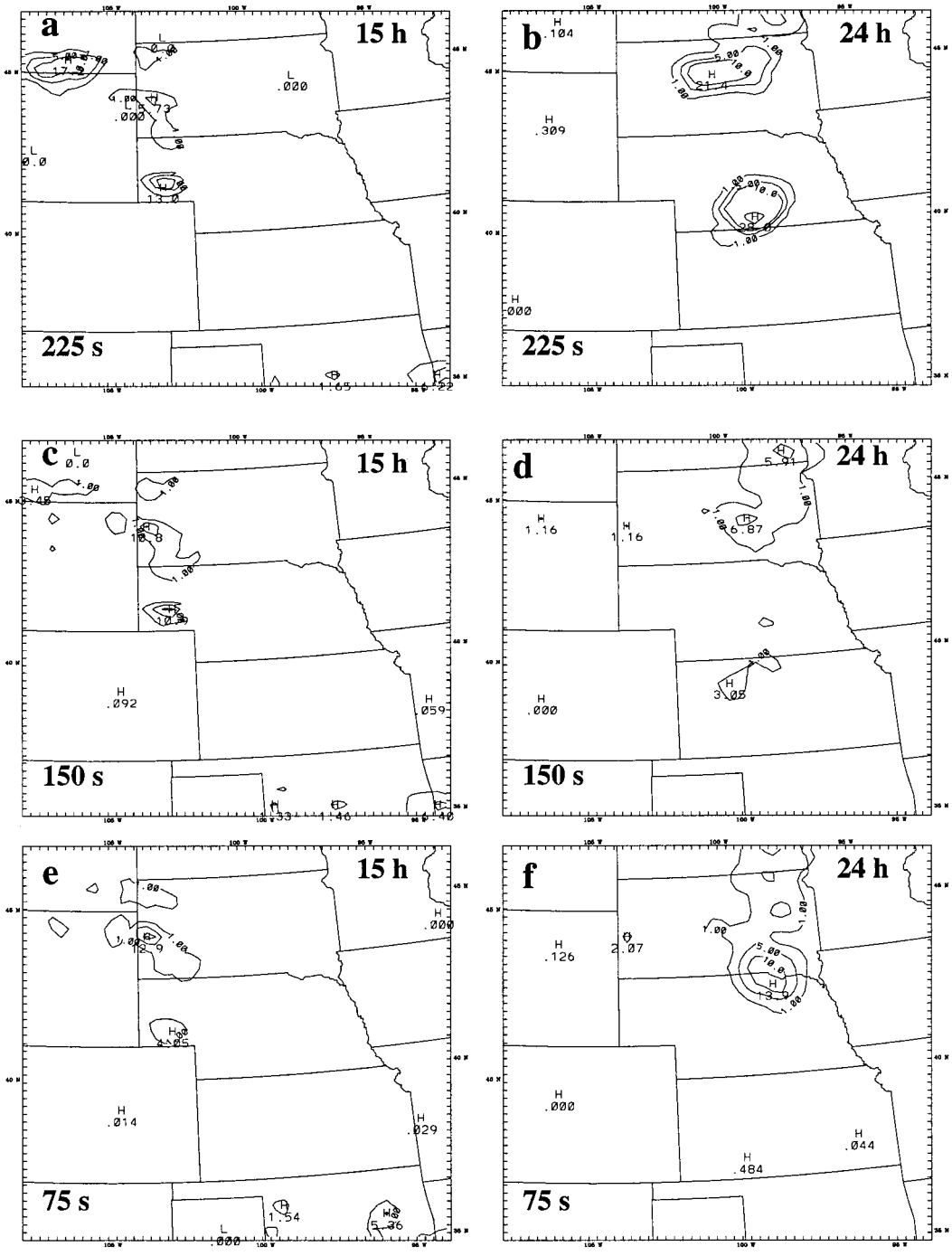

FIG. 6. The 3-h total precipitation fields at 15 and 24 h for the HYGR runs: (left panels) at 15 h and (right panels) at 24 h. Contours are at 1, 5, 10, and 25 mm.

time, and the other is related to the time step–dependent numerical terms such as the dissipation term. In MM5, the background horizontal diffusivity is set to be inversely proportional to the time step, for a reason to be explained in the next section. For the same MM5 configuration, therefore, a smaller time step corresponds to stronger horizontal background diffusion. In order to determine how much of the time step sensitivity in the MCS simulations has to do with the truncation error, one needs to examine model runs with time step–independent diffusivity.

For this purpose, we have conducted simulations using the same background horizontal diffusion for different time steps. For each of the three model config-

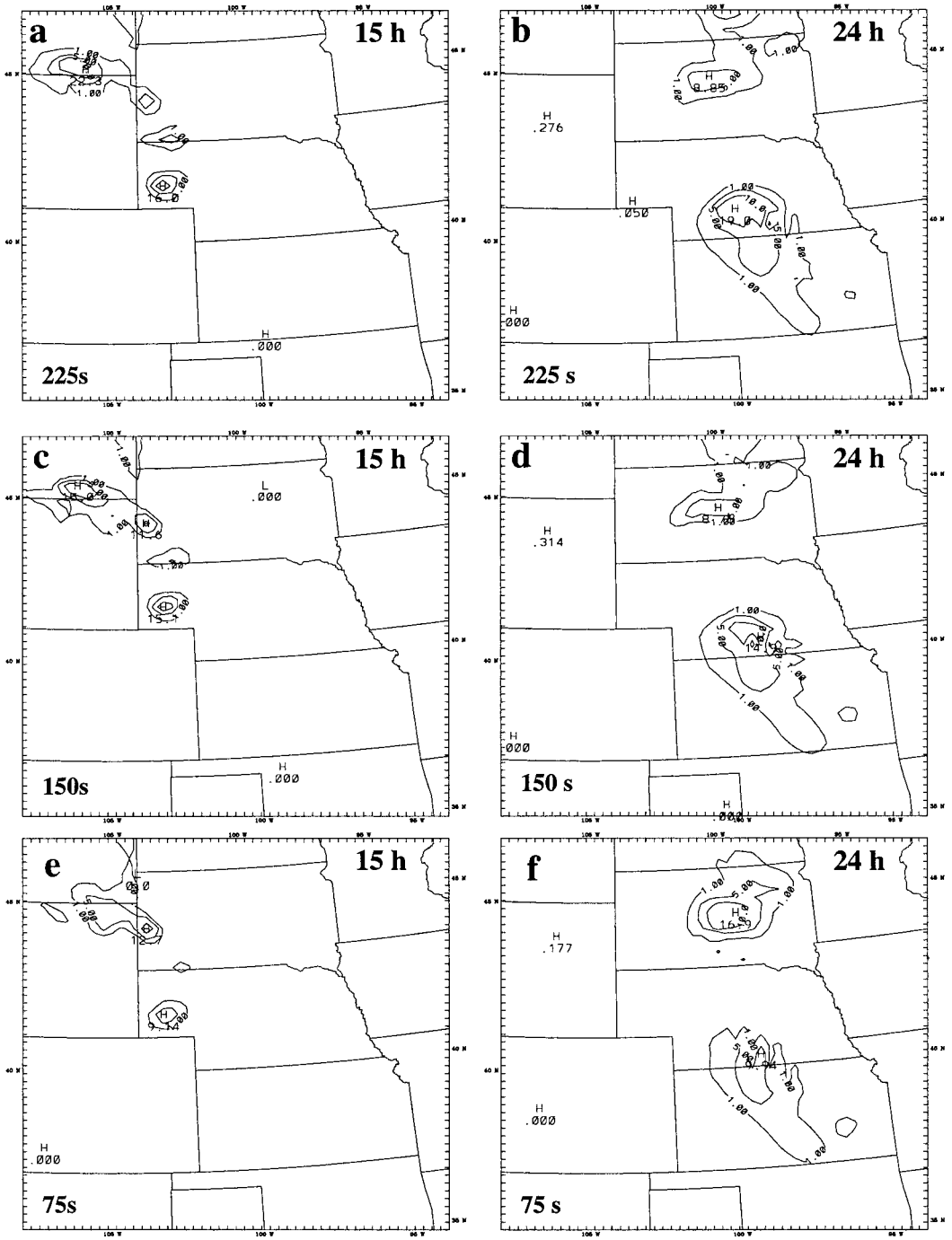

FIG. 7. The 3-h total precipitation fields at 15 h and 24 h for NHBM runs: (left panels) at 15 h and (right panels) at 24 h. Contours are at 1, 5, 10, and 25 mm.

urations, that is, HYGR, NHGR, and NHBM, two additional MM5 runs are performed using $\Delta t = 150$ s and $\Delta t = 75$ s, respectively, while keeping the background horizontal diffusivity the same as in the $\Delta t = 225$ s run. The precipitation fields at 24 h from these runs with constant background horizontal diffusivity are shown in Fig. 11 for the HYGR experiment, and in Fig. 12 for the NHBM experiment.

In all cases, the effect of time step size on MCS simulations is significantly smaller when the horizontal diffusivity is kept independent of the time step. The simulations of the southeastward-moving MCS improve

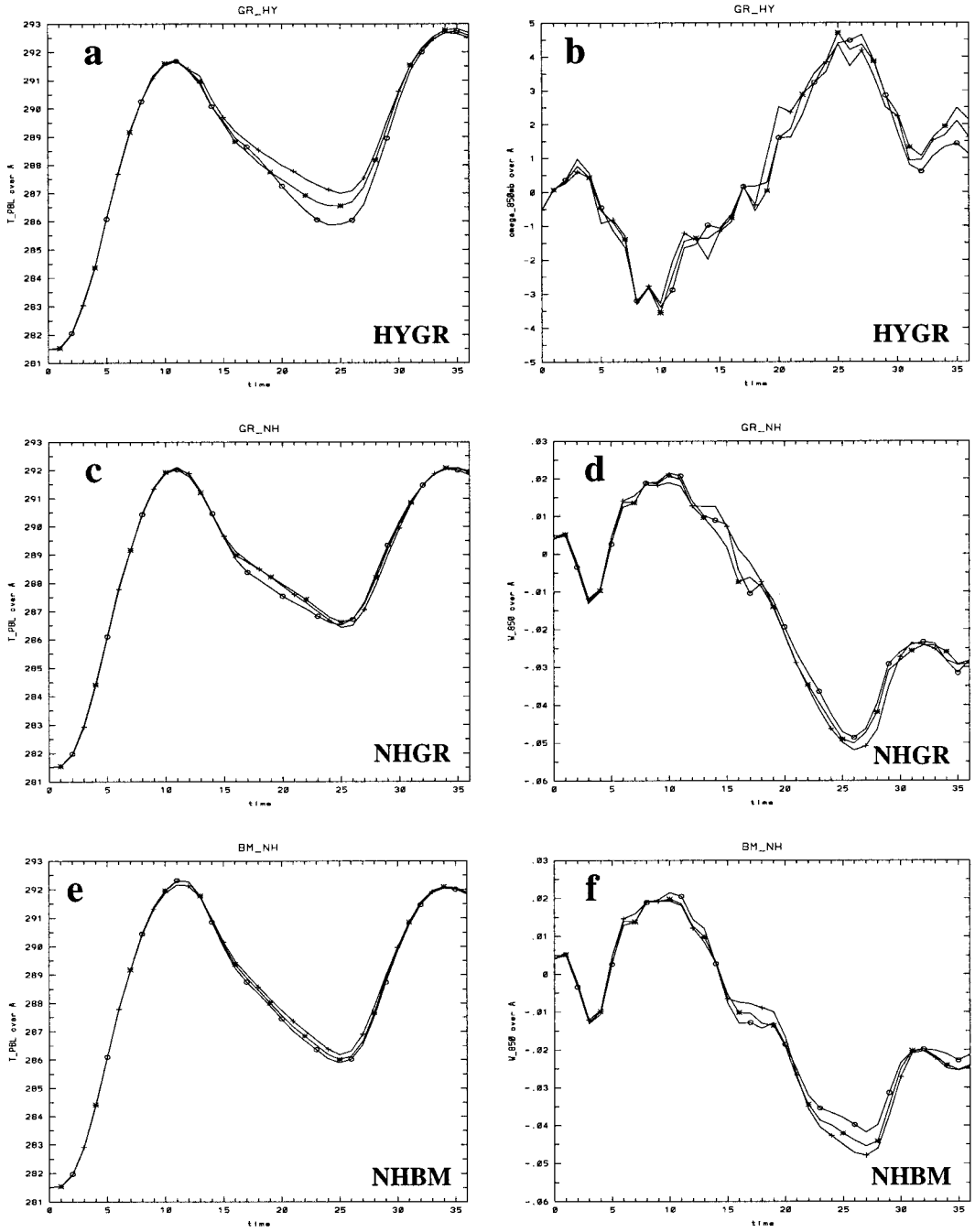

FIG. 8. The mean PBL temperature (K; left panels) and vertical motion at 850 hPa (m s^{-1}; right panels) in the area of convection initiation (A in Fig. 1) as a function of simulation time (h): ○, Δt = 225 s; *, Δt = 150 s; and +, Δt = 75 s.

significantly in HYGR150 and HYGR75 when a smaller background horizontal diffusivity corresponding to Δt = 225 s is used. In fact, while Figs. 9c and 9d show only one area of precipitation, Figs. 11c and 11d show two areas of precipitation due to two strong MCSs. The differences among HYGR75, HYGR150, and HYGR225 become much smaller when the same background horizontal diffusivity is used. Nevertheless, there still exist substantial differences among the HYGR runs, especially between HYGR150 and HYGR75, in terms of the MCS evolution and the rainfall amount produced by the MCSs in the mature and dissipating stages. This is true for both subgrid-scale and resolvable-scale precipitation. At 24 h in HYGR75, the northern system extends farther south, and the maximum rainfall amount decreases by 60% from HYGR150. Smaller

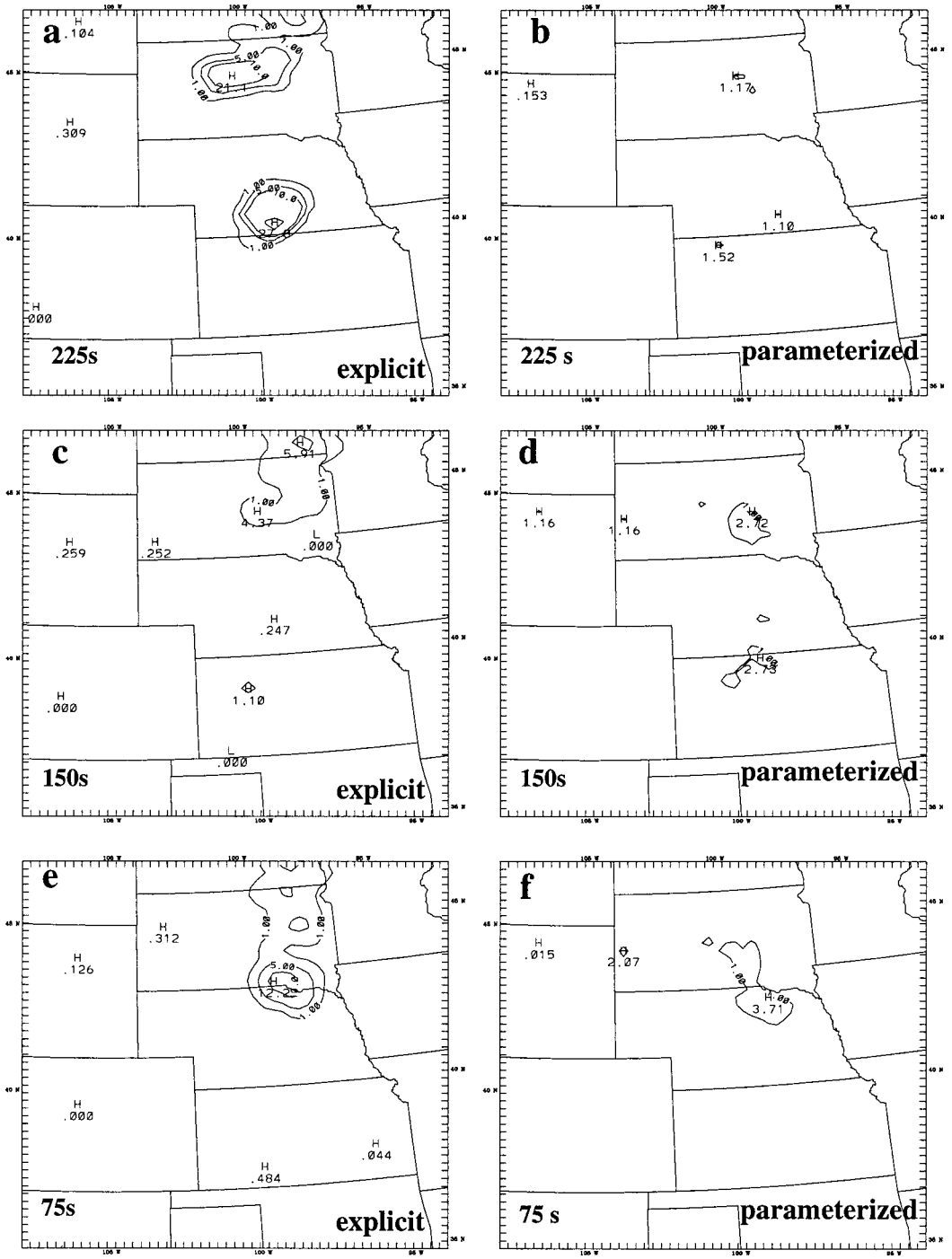

FIG. 9. The 3-h explicit and parameterized precipitation fields at 24 h for HYGR runs with (a), (b) Δt = 225 s, (c), (d) Δt = 150 s, and (e), (f) Δt = 75 s. Contours are at 1, 5, 10, and 25 mm.

differences are seen in the southeastward-moving MCS; at 24 h, the maximum rainfall rate in the southeastward-moving MCS is reduced by 15% as Δt is reduced from 225 to 150 s, and by another 20% when Δt is reduced from 150 to 75 s. Similar results also occur in the NHGR runs (not shown).

A constant background horizontal diffusivity also results in increased rainfall from the southeastward-moving MCS in the NHBM150 and NHBM75 runs, especially at resolvable scales (Figs. 12a,c). As with the HYGR simulations, the differences among the three NHBM runs are greatly reduced. In fact, only limited

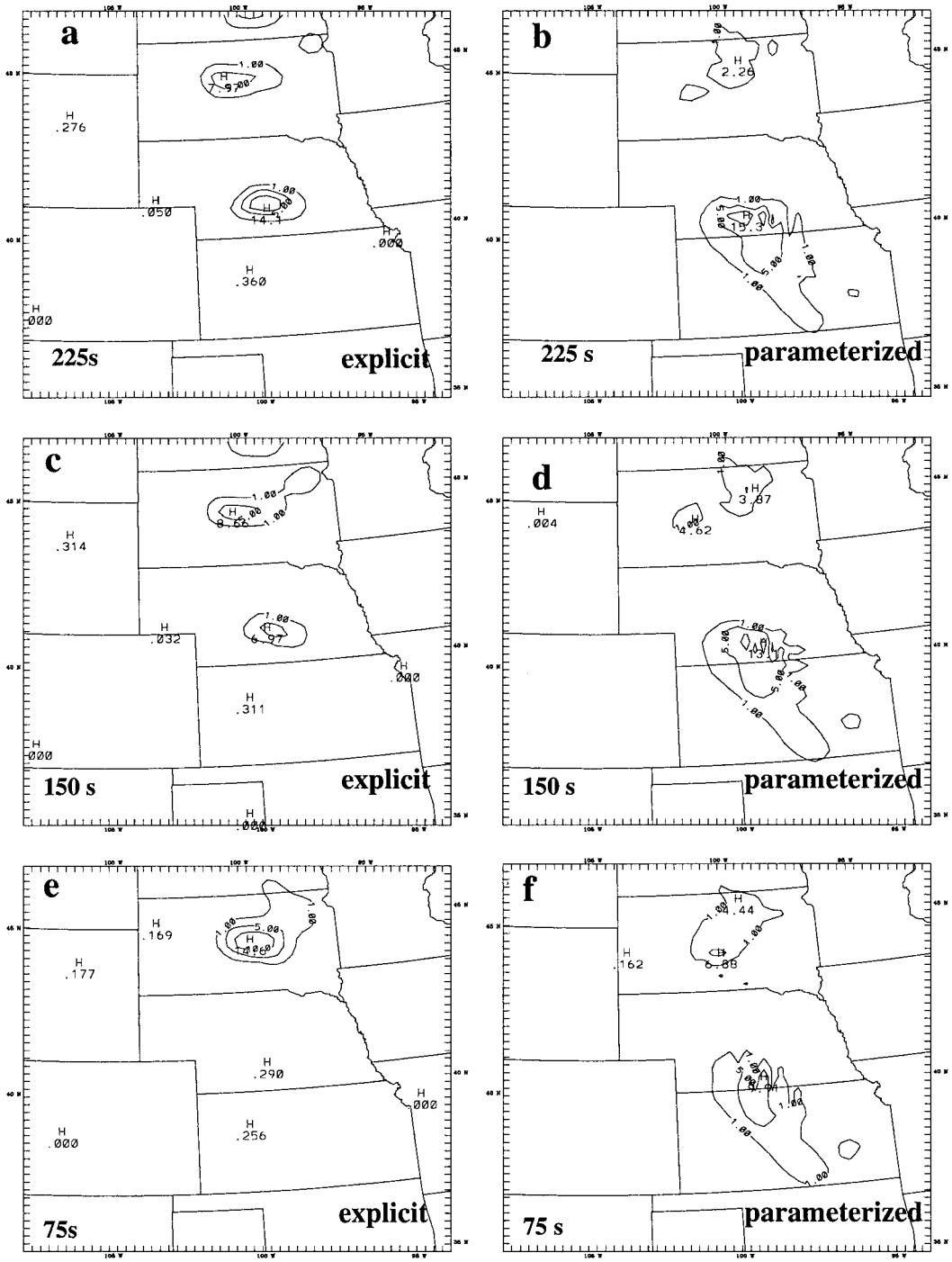

FIG. 10. The 3-h explicit and parameterized precipitation fields at 24 h for NHBM runs with (a), (b) $\Delta t = 225$ s, (c), (d) $\Delta t = 150$ s, and (e), (f) $\Delta t = 75$ s. Contours are at 1, 5, 10, and 25 mm.

quantitative differences still remain among the rainfall amounts throughout the simulations. At 24 h, the maximum change in the total rainfall is about 15% as the time step is changed from 225 to 150 s or from 150 to 75 s.

It appears that the sensitivity of MCS simulations to time step size is largely numerical, and can be significantly reduced by making the background diffusivity independent of time step size. Under that condition, the truncation errors due to different time step sizes cause mainly modest changes in the total rainfall amount. The effect of temporal truncation errors may or may not be

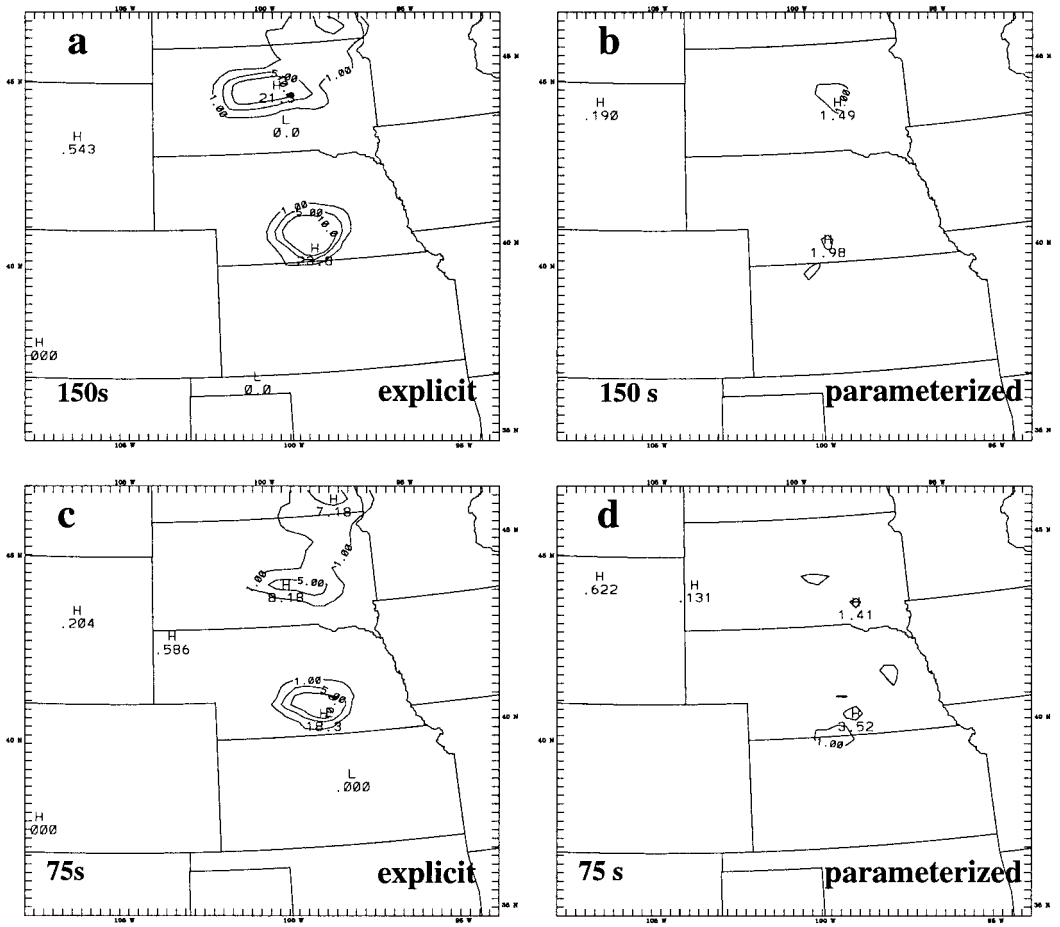

FIG. 11. The 3-h explicit and parameterized precipitation fields at 24 h for the HYGR runs using (a), (b) $\Delta t = 150$ s and (c), (d) $\Delta t = 75$ s, but keeping horizontal background diffusion the same as in HYGR225.

negligible, depending on the physics schemes used in the simulations and the stage of the MCS. The sensitivity to truncation errors seems to be larger in the experiments using the Grell CPS than in those using the Betts–Miller CPS.

6. Discussion

Mesoscale model experiments have been conducted to determine the effect of time step size in the simulations of MCSs. We have found that the simulation of an MCS in a weakly forced large-scale environment, although numerically stable, is sensitive to the time step size used in the model integration. Three experiments, using different model configurations, show contrasting sensitivities to the time step size.

Of the model variables examined, the precipitation field is the most sensitive to such changes. When the time step is decreased, both the intensity and location of convective development are affected. In particular, the precipitation amount in a region can change by more than 50% when the time step is reduced from 225 to 150 s. Other more basic model parameters, such as the PBL temperature and 850-hPa vertical motion in the area of convective initiation, change by small percentages as the time step is reduced, suggesting that they are less sensitive to time step changes.

It is found that a major part of the sensitivity to time step size is due to the time step dependence of the horizontal diffusivity. In a numerical model, horizontal diffusion is used to control the growth of nonlinear instability and suppress small-scale computational noise. The definition of the horizontal diffusion terms has always been empirical. In MM5, second-order diffusion is used adjacent to the coarse-domain boundaries and fourth-order diffusion is used at the other interior points.[1] The second-order diffusion coefficient K_H consists of a back-

[1] In addition to the numerical horizontal diffusion discussed in this section, MM5 also includes a second-order vertical diffusion term that parameterizes physical subgrid transport via mixing-length theory.

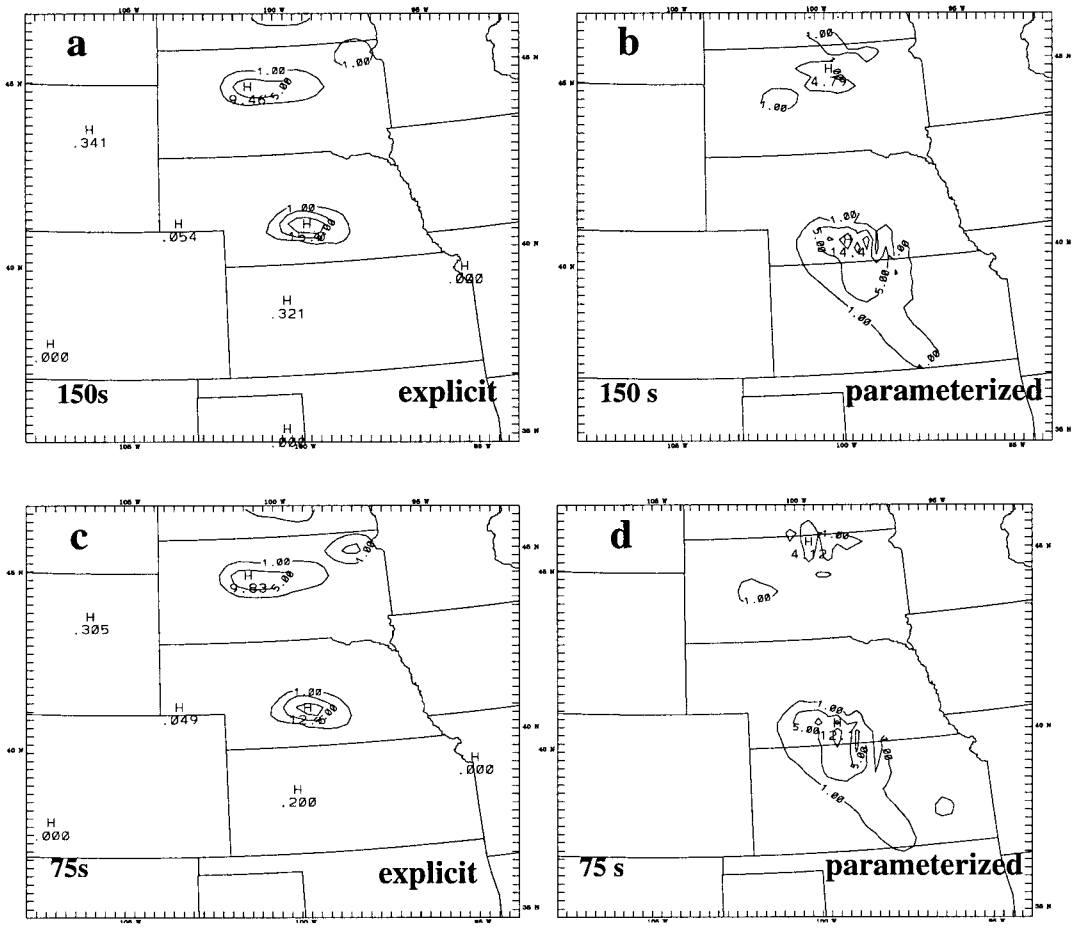

FIG. 12. The 3-h explicit and parameterized precipitation fields at 24 h for the NHBM runs using (a), (b) $\Delta t = 150$ s and (c), (d) $\Delta t = 75$ s, but keeping horizontal background diffusion the same as in NHBM225.

ground value K_{H0} plus a term proportional to the deformation

$$K_H = K_{H0} + 0.25\kappa^2(\Delta x)^2\left[\left(\frac{\partial u}{\partial x} - \frac{\partial v}{\partial y}\right)^2 + \left(\frac{\partial v}{\partial x} + \frac{\partial u}{\partial y}\right)^2\right]^{1/2}, \quad (1)$$

where

$$K_{H0} = 3.0 \times 10^{-3}\,(\Delta x)^2/\Delta t \quad (2)$$

and K_H has an upper limit of $(\Delta x)^2/(32\Delta t)$ (from the standard MM5, Version 2 code[2]). Here Δx is the horizontal grid increment and κ is the von Kármán constant. The fourth-order diffusion coefficient is $-K_H(\Delta x)^2$.

In the expression of K_H, the background term is time step dependent while the deformation-dependent part of K_H is not. In order to understand the relative importance of the background term and the deformation-dependent term in the total horizontal diffusion, we examined the magnitudes of the two terms in the model runs. The results show that the background term is dominant at all levels and locations throughout the simulation time. Figure 13 shows the domain-averaged ratio of the background term to the full horizontal diffusion coefficient for the NHBM225 and NHBM75 runs. The ratios decrease slowly with simulation time as the average flow deformation increases. However, the values are above 0.9 almost throughout the simulation time. That is, the background term is an order of magnitude larger than the deformation-dependent term.

The MM5 formulation of K_{H0} keeps a consistent damping rate with respect to the number of time steps across all grids in a simulation. Anthes and Warner (1978) have shown that the $n\Delta x$ wave damping rate D, in one time step, by the diffusion term is given by

$$D = 1 - (2K_H\Delta t/\Delta x^2)(1 - \cos 2\pi/n). \quad (3)$$

Therefore, K_{H0}, as given in (2), ensures that $2\Delta x$ waves would damp by the same percentage in a given number of time steps for all of the grids used in the model. However, as one decreases the time step size for the

[2] The coefficient before the deformation term in (1) and the upper limit of K_H given in Grell et al. (1994) are $0.5\kappa^2(\Delta x)^2$ and $(\Delta x)^2/(64\Delta t)$, respectively.

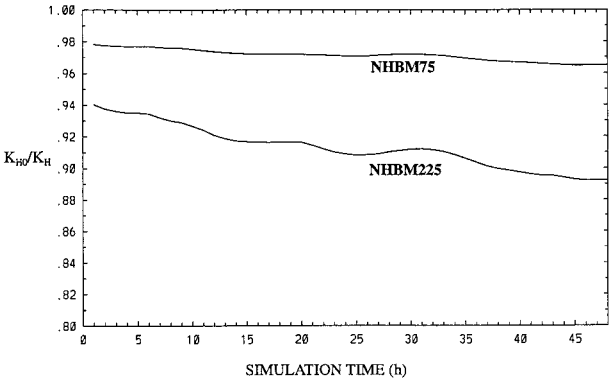

FIG. 13. The domain-averaged ratio of the background horizontal diffusion coefficient to the full horizontal diffusion coefficient for the NHBM225 and NHBM75 runs.

same Δx value, the damping becomes more rapid with time. Nevertheless, it is also consistent with the stability analysis of the linear second-order diffusion equation to define K_{H0} as proportional to $\Delta x^2/\Delta t$. When the linear second-order diffusion equation is discretized explicitly, the stability criterion is that $K_H\Delta t/\Delta x^2 < \frac{1}{2}$ (e.g., Haltiner and Williams 1980). Taking nonlinearity into account, it is natural to choose K_{H0} such that $K_{H0}\Delta t/\Delta x^2 = \text{constant} \ll 1$. Computational mixing terms of the same form are also suggested in the Advanced Regional Prediction System, though it is left to the users to supply the exact values of K_{H0} (Xue et al. 1995).

Although the background diffusion given in (2) is a numerically reasonable formulation, our results of MCS simulations seem to indicate excessive smoothing when the time step is small. One way to avoid this time step sensitivity may be to add an option for the background diffusion in MM5 to be set to $1.0\Delta x$, which is what one would get from (2) by assuming $\Delta t = 3\Delta x$ (Δx in km) and making the units agree. In this way, the diffusion would not be directly time step dependent within a given grid, but would change on the various grids. This could be added as a switch, such that the diffusion could be increased, as is now done, if one continues to have numerical instability problems.

In section 5, we have shown that when the diffusivity is made independent of the time step, the sensitivity of MCS simulations to time step size is significantly reduced. The remaining changes caused by the time step size may or may not be negligible, depending on the physics schemes used and the stage of the MCS simulation. There may be several sources of time step sensitivity other than truncation errors and numerical diffusivity. One possibility is the microphysics scheme, since there is a $1/\Delta t$ factor in the ice initiation and vapor condensation schemes used in MM5 (Rutledge and Hobbs 1983).

The model versions that use the Grell CPS appear to be more sensitive to the changes in prognostic variables than the versions that use the Betts–Miller CPS. Since the Grell CPS tends to quickly turn most of the precipitation generation over to the resolvable-scale microphysical scheme, while the Betts–Miller scheme often retains most of the precipitation as implicit, this could be an indication that the resolvable-scale microphysical scheme is more sensitive than the subgrid convective parameterization to the changes in prognostic variables caused by changing the time step size.

In summary, most of the sensitivity to Δt as shown in this paper can be regarded as the model's sensitivity to the size of the numerical horizontal diffusivity. The purpose of the numerical diffusivity in the model is to discourage the growth of nonlinear instability and to filter out very short waves that are often believed to be of spurious origin. This leads us to the conclusion that the simulations are sensitive to small perturbations of the model state under certain conditions. However, this sensitivity may not be entirely numerical. It may be realistic for MCS development when the forcing on large scales is weak, in which cases convective initiation may also appear as a small-scale perturbation. In such cases, the choice of a linearly stable model time step, in combination with a definition of the numerical diffusivity, may sometimes be as important as the choice of the basic model configurations such as the physics schemes and grid increment. For the case presented, the model results do not converge as the time step size is decreased, when the background horizontal diffusivity is set inversely proportional to the time step as is typically done in mesoscale models. This is yet another demonstration of the difficulty inherent in producing accurate QPFs.

The conclusions that can be drawn from this study apply only to a MCS-type event in a weakly forced large-scale environment, and should not be generalized too broadly. Preliminary tests using initial conditions from another case, in which an MCS developed under relatively strong large-scale forcing for upward motion, show much less time step dependency. On the other hand, there have been other encounters with model sensitivity to changes in time step, albeit not well documented. Using a cloud-resolving model, C.-H. Liu (NCAR 2000, personal communication) found noticeable sensitivity to time step size in the modeled precipitation, a trait not seen as clearly in other model variables.

Acknowledgments. The authors would like to thank Dr. Georg Grell for his helpful suggestions. This study was supported by the National Science Foundation under Grants ATM-9424397 and ATM-9501532. The MM5 simulations were produced on the NCAR Crays, and the support of both NCAR/SCD and NCAR/MMM is deeply appreciated. The Penn State–NCAR mesoscale modeling system is maintained by the efforts of many scientists at both institutions, and we are grateful for all their hard work and dedication to making this model easily accessible and user friendly.

REFERENCES

Anthes, R. A., and T. T. Warner, 1978: Development of hydrodynamic models suitable for air pollution and other mesometeorological studies. *Mon. Wea. Rev.*, **106,** 1045–1078.

Augustine, J. A., and K. W. Howard, 1988: Mesoscale convective complexes over the United States during 1985. *Mon. Wea. Rev.*, **116,** 685–701.

Benjamin, S. G., and N. L. Seaman, 1985: A simple scheme for objective analysis in curved flow. *Mon. Wea. Rev.,* **113,** 1184–1198.

Betts, A. K., and M. J. Miller, 1993: The Betts–Miller scheme. *The Representation of Cumulus Convection in Numerical Models, Meteor. Monogr.*, No. 46, Amer. Meteor. Soc., 107–121.

Blackadar, A. K., 1979: High resolution models of the planetary boundary layer. *Advances in Environmental Science and Engineering,* J. Pfafflin and E. Ziegler, Eds., Vol. 1, No. 1, Gordon and Breach, 50–85.

Dudhia, J., 1989: Numerical study of convection observed during the winter monsoon experiment using a mesoscale two-dimensional model. *J. Atmos. Sci.,* **46,** 3077–3107.

——, 1993: A nonhydrostatic version of the Penn State/NCAR mesoscale model: Validation tests and the simulation of an Atlantic cyclone and cold front. *Mon. Wea. Rev.,* **121,** 1493–1513.

Emanuel, K. A., and D. J. Raymond, 1992: Report from a workshop on cumulus parameterization Key Biscayne, Florida, 3–5 May 1991. *Bull. Amer. Meteor. Soc.,* **73,** 318–325.

Grell, G., 1993: Prognostic evaluation of assumptions used by cumulus parameterizations. *Mon. Wea. Rev.,* **121,** 764–787.

——, J. Dudhia, and D. R. Stauffer, 1994: A description of the fifth-generation Penn State/NCAR mesoscale model (MM5). NCAR Tech. Note NCAR/TN-398 + STR, 122 pp.

Haltiner, G. J., and R. T. Williams, 1980: *Numerical Prediction and Dynamic Meteorology*. 2d ed. Wiley, 477 pp.

Heideman, K. F., and J. M. Fritsch, 1988: Forcing mechanisms and other characteristics of significant summertime precipitation. *Wea. Forecasting,* **3,** 115–130.

Houze, R. A., Jr., 1993: *Cloud Dynamics.* Academic Press, 573 pp.

Janjic, Z. I., 1994: The step-mountain eta coordinate model: Further developments of the convection, viscous sublayer, and turbulence closure schemes. *Mon. Wea. Rev.,* **122,** 927–945.

Janssen, P. A., and J. D. Doyle, 1997: On spurious chaotic behavior in the discretized ECMWF physics scheme. ECMWF Tech. Memo. 234, 24 pp.

Kuo, Y.-H., R. J. Reed, and Y.-B. Liu, 1996: The ERICA IOP5 storm. Part III: Mesoscale cyclogenesis and precipitation parameterization. *Mon. Wea. Rev.,* **124,** 1409–1434.

Maddox, R. A., 1980: Mesoscale convective complexes. *Bull. Amer. Meteor. Soc.,* **61,** 1374–1387.

Mellor, G. L., and T. Yamada, 1982: Development of a turbulent closure model for geophysical fluid problems. *Rev. Geophys.,* **20,** 851–875.

Rutledge, S. A., and P. V. Hobbs, 1983: The mesoscale and microscale structure and organization of clouds and precipitation in midlatitude cyclones. VIII: A model for the ''seeder-feeder'' process in warm-frontal rainbands. *J. Atmos. Sci.,* **40,** 2949–2972.

Stensrud, D. J., and J. M. Fritsch, 1994a: Mesoscale convective systems in weakly forced large-scale environments. Part II: Generation of a mesoscale initial condition. *Mon. Wea. Rev.,* **122,** 2068–2083.

——, and ——, 1994b: Mesoscale convective systems in weakly forced large-scale environments. Part III: Numerical simulations and implications for operational forecasting. *Mon. Wea. Rev.,* **122,** 2084–2104.

——, J.-W. Bao, and T. T. Warner, 2000: Using initial condition and model physics perturbations in short-range ensemble simulations of mesoscale convective systems. *Mon. Wea. Rev.,* **128,** 2077–2107.

Walcek, C. J., 1994: Cloud cover and its relationship to relative humidity during a springtime midlatitude cyclone. *Mon. Wea. Rev.,* **122,** 1021–1035.

Wang, W., and N. L. Seaman, 1997: A comparison study of convective parameterization schemes in a mesoscale model. *Mon. Wea. Rev.,* **125,** 252–278.

Xue, M., K. K. Droegemeier, V. Wong, A. Shapiro, and K. Brewster, 1995: ARPS version 4.0 user's guide. Center for Analysis and Prediction of Storms, 380 pp [Available from CAPS, University of Oklahoma, Norman, OK 73019].

Zhang, D.-L., and R. A. Anthes, 1982: A high-resolution model of the planetary boundary layer—Sensitivity tests and comparisons with SESAME-79 data. *J. Appl. Meteor.,* **21,** 1594–1609.